LETTERS

100-metre-diameter moonlets in Saturn's A ring from observations of 'propeller' structures

Matthew S. Tiscareno[1], Joseph A. Burns[1,2], Matthew M. Hedman[1], Carolyn C. Porco[3], John W. Weiss[3], Luke Dones[4], Derek C. Richardson[5] & Carl D. Murray[6]

Saturn's main rings are composed predominantly of water-ice particles ranging between about 1 centimetre and 10 metres in radius. Above this size range, the number of particles drops sharply, according to the interpretation of spacecraft[1] and stellar[2] occultations. Other than the gap moons Pan and Daphnis (the provisional name of S/2005 S1), which have sizes of several kilometres, no individual bodies in the rings have been directly observed, and the population of ring particles larger than ten metres has been essentially unknown. Here we report the observation of four longitudinal double-streaks in an otherwise bland part of the mid-A ring. We infer that these 'propeller'-shaped perturbations[3–5] arise from the effects of embedded moonlets approximately 40 to 120 m in diameter. Direct observation of this phenomenon validates models of proto-planetary disks in which similar processes are posited[4,6]. A population of moonlets, as implied by the size distribution that we find, could help explain gaps in the more tenuous regions of the Cassini division and the C ring[7]. The existence of such large embedded moonlets is most naturally compatible with a ring originating in the break-up of a larger body[8–11], but accretion from a circumplanetary disk[12] is also plausible if subsequent growth onto large particles occurs after the primary accretion phase has concluded[13,14].

Four examples of a unique structure previously unseen in the rings were found in two images (Fig. 1) taken by the Imaging Science Subsystem (ISS) of the Cassini spacecraft. Each of these features is a symmetric double-streak, the individual lobes of which lie in the longitudinal (horizontal) direction, with a radial (vertical) offset between them. In each case, the lobe that is radially closer to Saturn also extends in the longitudinally leading direction (that is, in the direction of orbital motion). Supplementary Figs S1 and S2 display the full images, and their placement within the ring system is given in Supplementary Fig. S3.

'Propeller'-shaped structures, very similar to those visible here, have been predicted analytically[3,4] and simulated numerically[5]. Such disturbances[15,16] are produced when background ring particles are carried by the keplerian shear flow past a more massive compatriot. Moonlets larger than a few kilometres have been predicted[7,17] to clear gaps that extend the full circumference of the rings, just as Pan and Daphnis are seen to do. In contrast, the perturbations introduced by smaller moonlets are washed out as diffusive and viscous effects quickly fill in the disturbed region. For perturbing embedded moonlets of intermediate size—tens to hundreds of metres in radius—the resulting disturbance has two interwoven components: an S-shaped gap (with reduced, but non-zero, density), flanked by density enhancements generated similarly to the 'moonlet wakes' present on either side of the Encke and Keeler gaps[18–20].

The observed 'propeller' features are two to three times brighter than the background ring (see Fig. 2). Because the images under discussion show the unlit side of the rings, bright features may in principle be either more or less dense than the surrounding ring material (an entirely evacuated gap in the rings would scatter no light, and a completely opaque ring would transmit no light). Given previous measurements of the background optical depth in the mid-A ring[21,22], the near-nadir observing geometry for these images, and standard photometric models[23,24], we expect to find that bright features correspond to density enhancements. However, these models predict significantly lower contrast between dense and background regions than is observed. We note that Voyager images of the A ring similarly exhibited high contrast that could not be explained by standard photometric models[24]. Differences in ring thickness between the 'propeller' structure and the background ring may affect the photometric behaviour in unknown ways (especially considering the unique viewing geometry of these images). Furthermore, the presence of self-gravity wakes[15,25–27] pervading the surrounding ring should lower the background ring's optical depth, and hence brightness, from the standard model predictions. The absence of wakes in the perturbed 'propeller' regions may explain the increase in contrast.

Figure 2 plots the locations of the brightness enhancements seen in Fig. 1, from which we measure the mean radial position of each lobe and then the radial offset Δr. Although the perturber's radius is directly proportional to the radial separation between the gaps[5], such a relationship is less clear for the related density enhancements. Thus, although the radial offsets are measured with ~10% uncertainty, model dependence dominates the uncertainty in the inferred moonlet sizes. Our observations are consistent with moonlets of the order of 20–60 m in radius embedded in the A ring, with the larger sizes being inferred when the bright features are interpreted as gaps.

Figure 2 also shows longitudinal scans along the features, in which pixel brightnesses at the core of each double-streak are radially binned and summed. The profile has a steeper slope on the side facing the perturber, just as numerical simulations produce. The full longitudinal extent of the 'propeller' features is ~3 km. Radial scans across the features were also computed for these images (see Supplementary Fig. S4), and show symmetrical gaussian shapes with widths similar to the radial offsets.

The rings' dynamical viscosity can in principle be derived from the length of the 'propeller' features in the longitudinal direction (effectively, the time it takes for diffusive processes to 'fill in' the disturbance created by the moonlet). The viscosity is significantly influenced by self-gravity wakes[28], with a theoretically expected value of $\nu \approx 90\,\mathrm{cm^2\,s^{-1}}$ for this location in the rings ($a = 130,000$ km). However, the uncertain photometry (see above) hampers our efforts at obtaining a meaningful viscosity measurement in multiple ways. Not only does the bright/dark ambiguity leave the moonlet's size

[1]Department of Astronomy, Cornell University, [2]Department of Theoretical and Applied Mechanics, Cornell University, Ithaca, New York 14853, USA. [3]CICLOPS, Space Science Institute, 4750 Walnut Street, Boulder, Colorado 80301, USA. [4]Southwest Research Institute, 1050 Walnut Street, Boulder, Colorado 80302, USA. [5]Department of Astronomy, University of Maryland, College Park, Maryland 20742, USA. [6]Astronomy Unit, Queen Mary, University of London, Mile End Road, E1 4NS, UK.
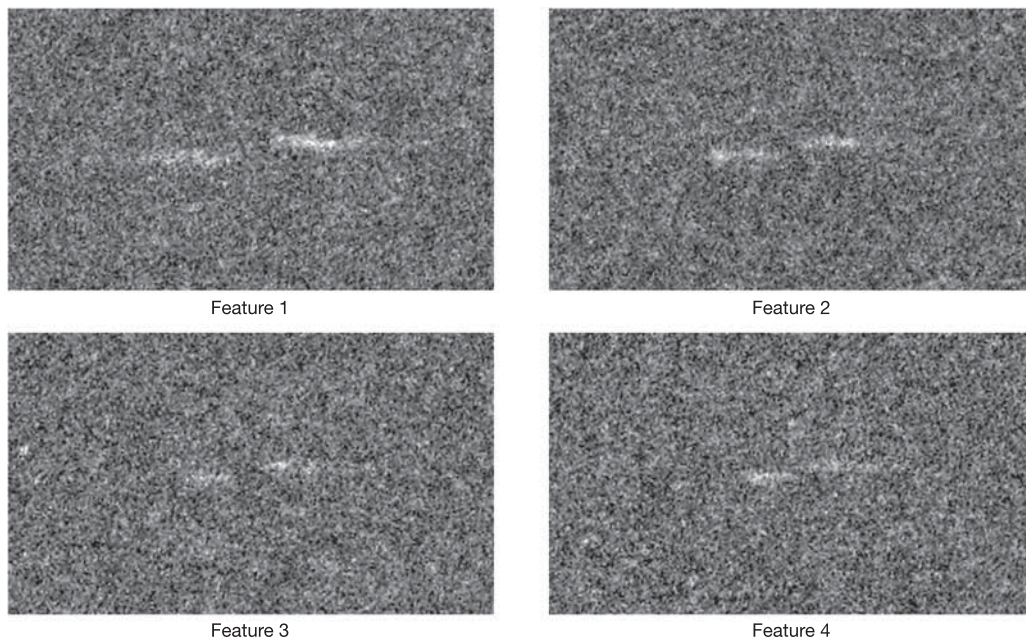
Figure 1 | Four longitudinally aligned double-streaks observed in a bland region of Saturn's A ring by the Cassini ISS camera. These are interpreted to be regions perturbed by unseen embedded moonlets located centrally between the streaks. The images have been cropped and reprojected, so that orbital motion is to the right, and Saturn's direction (radially inward) is up. In each of the four cases, the upper right-hand streak is closer to Saturn and orbitally leads the unseen moon. Cassini images N1467347210 (feature 1) and N1467347249 (features 2–4), seen in their entirety as Supplementary Figs S1 and S2, are the highest-resolution ring images yet obtained by

Cassini, and were taken during the spacecraft's insertion into Saturn orbit[19] on 1 July 2004. The images were calibrated using standard techniques[30] to convert discrete pixel data numbers to units of brightness divided by the solar flux (I/F). Residual horizontal banding (on the level of a few data numbers) was removed by horizontally averaging pixels away from the features of interest. The nominal image resolution is 52 m per pixel, and smearing due to keplerian motion of ring particles amounts to less than three pixels.

uncertain, but it is similarly difficult to calibrate absolutely the optical depth at which our data fall below the noise level. With plausible assumptions on these matters, our observations imply that ν ranges from $\sim 0.1\ \mathrm{cm^2\,s^{-1}}$ to $\sim 700\ \mathrm{cm^2\,s^{-1}}$.

Since four objects were found in a pair of images covering 2,800 km² apiece, we estimate the surface number density of moonlets

approximately 50 m in radius in weakly perturbed portions of the A ring to be $7 \times 10^{-4}\ \mathrm{km^{-2}}$. The total surface area of the A ring is $\sim 1.2 \times 10^{10}\ \mathrm{km^2}$, giving an estimated population (perhaps a primordial population, later altered in the more perturbed regions) of some 10^7 moonlets of this size. This calculation does not include two other images of similar resolution taken in the same sequence, in
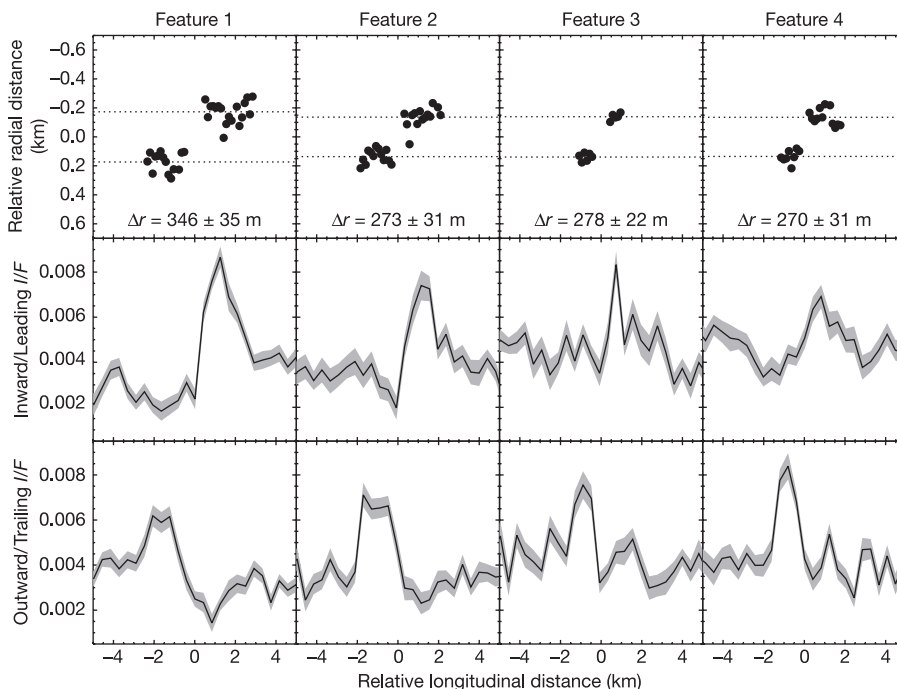
Figure 2 | Peak locations and longitudinal scans of the four double-streaks in Fig. 1. Top row, the radial locations of the brightest part of each feature, as a function of longitudinal distance relative to the inferred moon, are found by a gaussian fit to the total brightness. To increase the quality of each fit, resolution was lowered to 260 m in the longitudinal direction. We discarded four of the 90 data points because the gaussian's centre fell on a point of noise rather than the point of interest. Note the radial offset between the peaks of the outer and inner lobes. Dotted lines show the mean values for each lobe, and the radial offset between them, Δr, is given in each panel. Middle row, longitudinal scans of the brightness I/F along the radius of the inner lobe of each double-streak. The grey regions surrounding the solid lines denote the standard deviation of the mean value of the pixels in each bin. Bottom row, longitudinal scans of I/F along the radius of the outer lobe of each double-streak. We note that the longitudinal profiles are generally steeper on the side facing the moonlet.
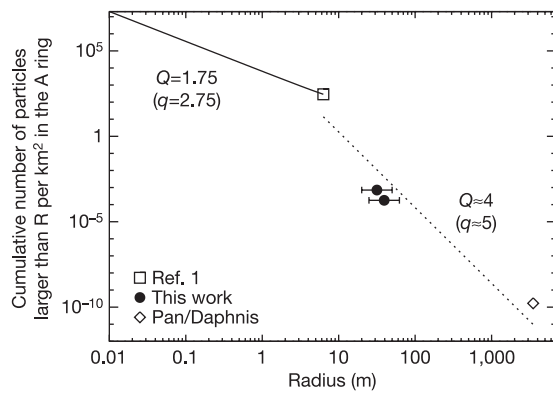
Figure 3 | Cumulative size distribution for particles in the A ring. The solid line and open square are calculated from Voyager radio occultations[1]; solid circles denote the moonlets announced in this work, with the plotted error bars indicating the model-dependent uncertainties (the range of possible radii) in their sizes; the open diamond indicates the two known ring moons Pan and Daphnis. The fitted cumulative power law for particles over ten metres in size (dotted line) has an index $Q = 4 \pm 1$. This 1σ uncertainty of ± 1 comes from linear regression using the moonlet size that gives the highest residuals, thus accounting for the model-dependent uncertainties. For a differential power law, such as is discussed in the main text, this corresponds to $q = Q + 1 = 5$.

which no features of this kind were found; we attribute this lack to the stronger density waves[13] present in those regions, which probably modify the moonlet population.

These findings allow us to extend previous estimates of the size distribution of particles in Saturn's rings. Interpretations of occultations of Voyager radio signals[1] and stars[2] have inferred a differential power-law distribution, $dn(R) \approx R^{-q}$ (where dn is the number of particles per unit area with radius R in the differential bin dR), with $2.7 < q < 3$ for centimetre-size to metre-size particles[1,29]. For larger particles, however, the distribution falls quite steeply. Figure 3 shows that the present results provide a 'missing link' between the largest particles observable by occultations ($r \approx 10$ m) and the two ring moons Pan and Daphnis ($r > \sim 3.5$ km). This analysis allows us to estimate a differential power-law index $q = 5 \pm 1$ over the range 10 m $< r < 3$ km.

The lack of similar features caused by even smaller moonlets can be attributed to the insignificant amplitudes expected in their density modulations, making them difficult to discern in these noisy images despite nominally sufficient spatial resolution. 'Propellers' too tiny to be resolved in an image would create an asymmetric profile in the noise; a preliminary search for such a profile has been unsuccessful. The current non-detection of larger moonlets ($r > \sim 100$ m) may be attributed to their rarity, as implied by the steep power-law size distribution; such features will be sought in planned lower-resolution images.

The present discovery indicates that the moons Pan and Daphnis are not isolated anomalies; rather, they are the endmembers in a continuous population of ring particles and embedded moonlets with a steep power-law size distribution. The largest bodies expected from direct accretion are on the order of the Toomre scale length, $L \approx 10$ m for the A ring[13], though subsequent accretion of ring particles may produce larger sizes[14,27], whereas particles up to 5 km in radius will result from the break-up of a larger moon[8]. Thus, a population of embedded moonlets 100 m in diameter will place an important constraint on the origin of Saturn's rings.

1. Zebker, H. A., Marouf, E. A. & Tyler, G. L. Saturn's rings: Particle size distributions for thin layer models. *Icarus* **64**, 531–548 (1985).
2. French, R. G. & Nicholson, P. D. Saturn's rings II. Particle sizes inferred from stellar occultation data. *Icarus* **145**, 502–523 (2000).
3. Spahn, F. & Sremcevic, M. Density patterns induced by small moonlets in Saturn's rings? *Astron. Astrophys.* **358**, 368–372 (2000).
4. Sremcevic, M., Spahn, F. & Duschl, W. J. Density structures in perturbed thin cold discs. *Mon. Not. R. Astron. Soc.* **337**, 1139–1152 (2002).
5. Seiss, M., Spahn, F., Sremcevic, M. & Salo, H. Structures induced by small moonlets in Saturn's rings: Implications for the Cassini Mission. *Geophys. Res. Lett.* **32**, L11205, doi:10.1029/2005GL022506 (2005).
6. Bryden, G., Chen, X., Lin, D. N. C., Nelson, R. P. & Papaloizou, J. C. B. Tidally induced gap formation in protostellar disks: gap clearing and suppression of protoplanetary growth. *Astrophys. J.* **514**, 344–367 (1999).
7. Lissauer, J. J., Shu, F. H. & Cuzzi, J. N. Moonlets in Saturn's rings? *Nature* **292**, 707–711 (1981).
8. Harris, A. W. in *Planetary Rings* (eds Greenberg, R. & Brahic, A.) 641–659 (Univ. Arizona Press, Tucson, 1984).
9. Dones, L. A recent cometary origin for Saturn's rings? *Icarus* **92**, 194–203 (1991).
10. Smith, B. A. *et al.* A new look at the Saturn system—the Voyager 2 images. *Science* **215**, 504–537 (1982).
11. Colwell, J. E. The disruption of planetary satellites and the creation of planetary rings. *Planet. Space Sci.* **42**, 1139–1149 (1994).
12. Pollack, J. B. The rings of Saturn. *Space Sci. Rev.* **18**, 3–93 (1975).
13. Shu, F. H. in *Planetary Rings* (eds Greenberg, R. & Brahic, A.) 513–561 (Univ. Arizona Press, Tucson, 1984).
14. Weidenschilling, S. J., Chapman, C. R., Davis, D. & Greenberg, R. in *Planetary Rings* (eds Greenberg, R. & Brahic, A.) 367–415 (Univ. Arizona Press, Tucson, 1984).
15. Julian, W. H. & Toomre, A. Non-axisymmetric responses of differentially rotating disks of stars. *Astrophys. J.* **146**, 810–827 (1966).
16. Murray, C. D. & Dermott, S. F. *Solar System Dynamics* (Cambridge Univ. Press, 1999).
17. Hénon, M. A simple model of Saturn's rings. *Nature* **293**, 33–35 (1981).
18. Showalter, M. R., Cuzzi, J. N., Marouf, E. A. & Esposito, L. W. Satellite 'wakes' and the orbit of the Encke Gap moonlet. *Icarus* **66**, 297–323 (1986).
19. Porco, C. C. *et al.* Cassini Imaging Science: initial results on Saturn's rings and small satellites. *Science* **307**, 1226–1236 (2005).
20. Lewis, M. C. & Stewart, G. R. Expectations for Cassini observations of ring material with nearby moons. *Icarus* **178**, 124–143 (2005).
21. Esposito, L. A., O'Callahan, M. & West, R. A. The structure of Saturn's rings: Implications from the Voyager stellar occultation. *Icarus* **56**, 439–452 (1983).
22. Nicholson, P. D. *et al.* Saturn's rings I. Optical depth profiles from the 28 Sgr occultation. *Icarus* **145**, 474–501 (2000).
23. Cuzzi, J. N. *et al.* in *Planetary Rings* (eds Greenberg, R. & Brahic, A.) 73–199 (Univ. Arizona Press, Tucson, 1984).
24. Dones, L., Cuzzi, J. N. & Showalter, M. R. Voyager photometry of Saturn's A ring. *Icarus* **105**, 184–215 (1993).
25. Dones, L. & Porco, C. C. Spiral density wakes in Saturn's A Ring? *Bull. Am. Astron. Soc.* **21**, 929 (1989).
26. Salo, H. Simulations of dense planetary rings III. Self-gravitating identical particles. *Icarus* **117**, 287–312 (1995).
27. Karjalainen, R. & Salo, H. Gravitational accretion of particles in Saturn's rings. *Icarus* **172**, 328–348 (2004).
28. Daisaka, H., Tanaka, H. & Ida, S. Viscosity in a dense planetary ring with self-gravitating particles. *Icarus* **154**, 296–312 (2001).
29. Showalter, M. R. & Nicholson, P. D. Saturn's rings through a microscope—particle size constraints from the Voyager PPS scan. *Icarus* **87**, 285–306 (1990).
30. Porco, C. C. *et al.* Cassini Imaging Science: instrument characteristics and anticipated scientific investigations at Saturn. *Space Sci. Rev.* **115**, 363–497 (2004).

Author Information Reprints and permissions information is available at npg.nature.com/reprintsandpermissions. The authors declare no competing financial interests. Correspondence and requests for materials should be addressed to M.S.T. (matthewt@astro.cornell.edu).